Hamburger Beiträge
zur Angewandten Mathematik

Convexity Rule for Shape Decomposition Based on Contour Evolution Hierarchy

Longin Jan Latecki and Rolf Lakämper

Reihe A
Preprint 133
January 1998

Hamburger Beiträge zur Angewandten Mathematik

Reihe A	Preprints
Reihe B	Berichte
Reihe C	Mathematische Modelle und Simulation
Reihe D	Elektrische Netzwerke und Bauelemente
Reihe E	Scientific Computing
Reihe F	Computational Fluid Dynamics and Data Analysis

Convexity Rule for Shape Decomposition Based on Contour Evolution Hierarchy

Longin Jan Latecki and Rolf Lakämper
Dept. of Applied Mathematics, University of Hamburg,
Bundesstr. 55, 20146 Hamburg, Germany
Emails: {latecki, lakaemper}@math.uni-hamburg.de

January 14, 1998

Abstract

We concentrate here on decomposition of 2D objects into meaningful *parts of visual form*, shortly *visual parts*. It is a simple observation that convex parts of objects determine visual parts. However, the problem is that many significant visual parts are not convex, since a visual part may have concavities. We solve this problem by identifying convex parts at different stages of a proposed **contour evolution** method in which significant visual parts will become convex object parts at higher stages of the evolution. We obtain a novel rule for decomposition of 2D objects into visual parts, called **hierarchical convexity rule**, which states that visual parts are enclosed by maximal convex (with respect to the object) boundary arcs at different stages of the contour evolution. Observe that this rule determines not only parts of boundary curves but directly the visual parts of objects. Moreover, the stages of the evolution hierarchy induce a hierarchical structure of the visual parts. The more advanced the stage of contour evolution, the more significant is the shape contribution of the obtained visual parts.

Keywords:

visual parts, curve evolution, digital curves, digital straight line segments,
total curvature, shape hierarchy, digital geometry

1 Introduction

We concentrate here on decomposition of 2D objects into meaningful parts. According to Siddiqi et al. [17],

> "*Part-based representations allow for recognition that is robust in the presence of occlusion, movement, deletion, or growth of portions of an object. In the task of forming high-level object-centered models from low-level image-based features, parts serve as an intermediate representation.*"

There is also a strong evidence for part-based representations in human vision, see [17] for an overview. Hoffman and Richards [9] provide a strong evidence that contours are psychologically segmented at negative curvature minima. They state the following rule (cited from Hoffman and Singh [10]):

> "**Minima rule for silhouettes:** *For any silhouette, all negative minima of curvature of its bounding curve are boundaries between parts.*"

Hoffman and Singh write [10]:

> "*... the minima rule states in principle what these boundaries are, leaving open how in practice they may be computed from images despite noise and other resources.*"

One of the main motivations for our work was the question how to robustly compute significant parts of boundaries from real digital images. In particular, since negative minima of curvature as well as other extremal points are obtained by local computation, their computation is not robust in real digital images.

Since objects we deal with in computer vision are mostly digital objects obtained by segmentation in digital images, our starting point was the discrete nature of digital objects. Therefore, we propose a multiscale shape decomposition rule which yields for many objects similar parts as in Hoffman and Richards [9]. However, we do not use extremal points of contour curves to compute the parts.

The presented approach to multiscale shape decomposition is based on shape hierarchy obtained by a curve evolution. We present a novel approach to evolution of digital planar curves that is based on digital linearization. In contrary to continuous curves, every digital curve is composed of digital line segments, i.e., every curve in a digital image is a digital polygonal curve. We decompose a digital curve into maximal digital line segments. The basic idea of the evolution is very simple: in every evolution step, we substitute two consecutive line segments with a single line segments joining their endpoints. The key property of the evolution is the order of this substitution. If we do this in the "right" order, then we obtain an intuitive shape evolution of the curve. The substitution is done according to a relevance order of digital arcs that measures the significance of their contribution to the shape of the curve, beginning with arcs that contribute in the less significant way. This method allows us first to eliminate noise influence without changing the shape of objects. For example, compare the original curve (a) to curve (b) in Figure 1.

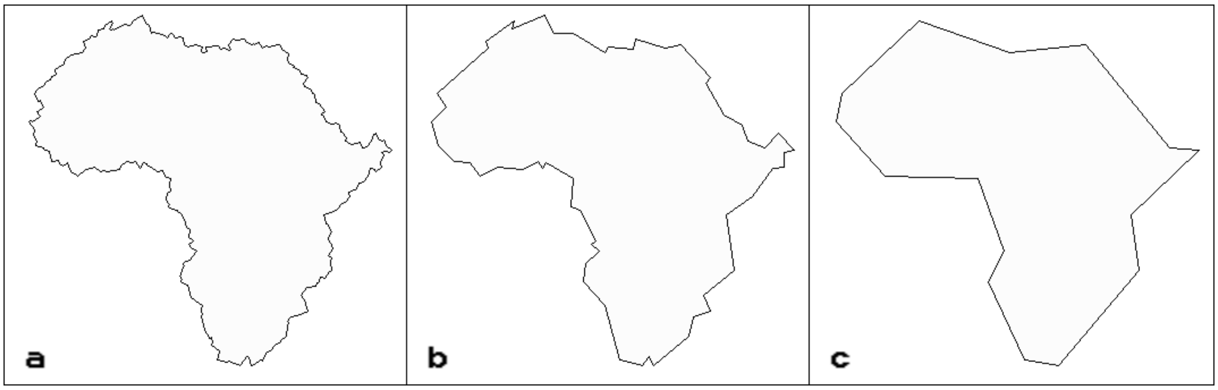

Figure 1: Curve evolution leads to a shape hierarchy: (c)>(b)>(c). (a) $\rightarrow$ (b): noise elimination, (b) $\rightarrow$ (c): shape simplification.

If we continue to evolve the curve, we will linearize digital arcs that are relevant for the curve shape, which will result in a successive simplification of the curve shape. We use this shape simplification to derive a shape hierarchy for planar curves. For example, Figure 1(c) shows one of the higher levels of the shape hierarchy of the object in Figure 1(a). Since in every evolution step, the number of digital line segments in the curve decomposition decreases by one, the evolution converges to a convex polygon, which defines the highest level in the shape hierarchy. The presented evolution method is translation, rotation, reflection and scaling invariant.

The obtained shape hierarchy is a base for object decomposition into relevant visual parts. The parts obtained on the highest levels of the hierarchy determine the most significant parts of the object.

To decompose a digital curve into relevant parts on a given level of the shape hierarchy, we group the digital line segments of its boundary curve into maximal convex arcs, which we will call **supported** arcs following Latecki and Rosenfeld [13]). We will call finite unions of supported arcs **tame** arcs. Maximal supported arcs determine alternating and overlapping convex and concave parts of the object boundary. For example, Figure 2 shows a decomposition of a polygonal curve into maximal supported arcs: the dashed arcs (inside the polygon) indicate the concave arcs with respect to the polygon while the dotted arcs (outside of the polygon) indicate the convex arcs with respect to the polygon. In the following, the term **maximal convex arc** denotes a supported arc that is convex with respect to the object.

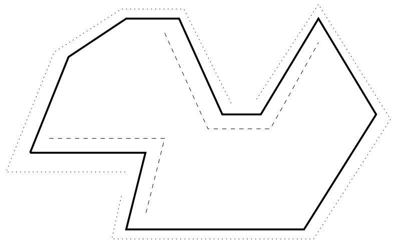

Figure 2: Decomposition of a polygonal arc into maximal supported arcs.

2 Shape Decomposition

We base our approach to shape decomposition into visual parts on the following simple and natural rule:

- **Hierarchical convexity rule:**
  The maximal convex arcs (with respect to the object) of the evolved contours determine parts of object boundary that enclose visual parts of the object. The relevance of the parts depends on the level of the evolution hierarchy and on the relevance of the convex arcs.

This rule is natural, since convex parts of objects clearly determine visual parts. However, the problem is that many significant visual parts are not convex. This problems is solved in our approach by the evolution hierarchy, since a significant visual part will become a convex part at a higher level of the evolution. This is due to the properties of the proposed evolution method. A significant visual part may have concavities, whose boundary parts are supported concave arcs. Since these concave arcs contribute in a less relevant way to the shape of the object than the boundary arc enclosing the significant visual part, the concavities will disappear in an earlier stage of the boundary evolution. Thus, there exists an evolution stage at which a significant visual part is a convex part.

Figure 3 shows two examples of the boundary and object parts obtained by the proposed hierarchical convexity rule. On the highest level of the shape hierarchy (a) in Figure 3, the evolved silhouette of the "bear" is decomposed into three maximal convex arcs, and the evolved silhouette of the "fish" is decomposed into two maximal convex arcs. The visual parts enclosed by these arcs represent the most relevant object parts, those are the fish body and the tail for the fish, and the upper body and legs together with hips for the bear. On one of the lower levels of the shape hierarchy (b) in Figure 3, we obtain further visual parts, e.g., the head and the arms for the bear. The visual parts obtained by the hierarchical convexity rule on levels (a) and (b) are shown in (c) projected on the original contours. Another example is given in Figure 6, where the order of pictures follows the steps of the evolution. For the shape hierarchy, we have the order: (f)>(e)>(d).

The shape hierarchy obtained by the evolution of a boundary curve induces a hierarchical structure of the visual parts:

- The lower is the level of the evolutional shape hierarchy, the less significant for the object shape are the parts determined.
- The parts obtained on a higher level of the shape hierarchy are inherited to the lower levels.

This means that on a lower level only the inherited parts are further divided. For example, on the level (b) in Figure 3, only the parts obtained on level (a) are further divided, e.g., the upper body of the bear is divided into the head and arms.

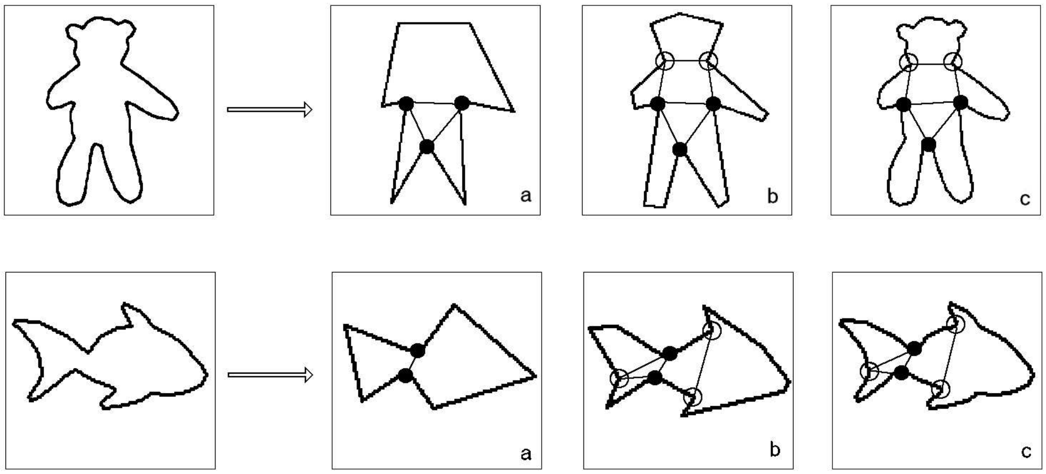

Figure 3: The object parts obtained on different levels of the evolution of the boundary curve.

The parts of boundaries obtained by the hierarchical convexity rule correspond for many objects to the parts obtained using points of minimal negative curvature (Hoffman and Richards [9]), see Figures 3 and 4, for example. This is the case when the endpoints of convex arcs are located near the points of minimal negative curvature. Also for many objects, the obtained parts of objects correspond to limbs and necks in the theory of Siddiqi and Kimia [16]. For boundaries of continuous objects, the endpoints of maximal convex arcs correspond to inflection points (e.g., inflection points are used for shape description in Freeman [4]). The correspondence of the endpoints of maximal convex arcs to different kinds of critical points (in the sense of differential geometry) is possible, since we work in a digital space which does not exactly follow the rules of differential geometry.

In our approach, we do not need to decide which points of minimal negative curvature have to be joint together in order to obtain object parts. The object parts obtained by joining two negative curvature minima are called *part cats* (Beusmans et al. [3]). As argumented in Hoffman and Singh [10], a separate theory is necessary to determine the part cats knowing the boundary points of minimal negative curvature.

- In our approach, the part cats are automatically determined by maximal convex arcs.

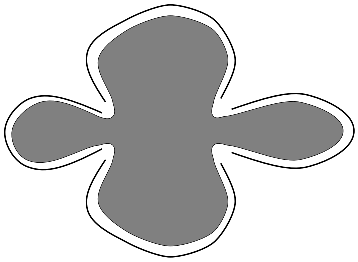

Figure 4: The parts obtained by the hierarchical convexity rule correspond to the parts obtained by points of minimal negative curvature.

Our approach allows us additionally

- to give a relevance measure for an obtained part that is based on the level of the shape hierarchy and on relevance of the maximal convex arc,
- to obtain a shape decomposition stable with respect to noise, due to the levels of the shape hierarchy and due to the fact that the convex arcs represent global properties of object boundaries.

The stability of the shape decomposition with respect to noise is due to the evolution process guided by the relevance order (described in more details in Section 3) and due to the fact that recognition of supported arcs is based on global features that are significantly less influenced by noise than locally defined points of minimal negative curvature. The stability is demonstrated in Figure 5. Although the original contour of the fish is distorted by two different levels of noise, the obtained parts are the same as for the original fish in Figure 3.

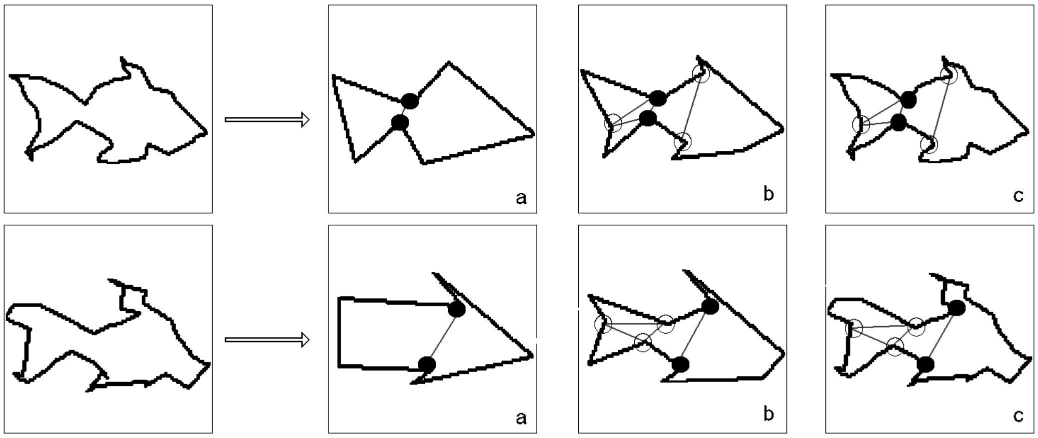

Figure 5: The proposed decomposition into visual parts is stable with respect to contour distortions.

In our approach, we can derive a relevance measure of visual parts from the relevance measure of supported arcs, i.e. the relevance measure of visual parts is based on the relevance of the contribution of the maximal convex arcs by which they are determined to the object shape, which depends on the total turn (i.e., global curvature) and the length that is normalized with respect to the total length of the boundary curve (see Section 4). Additionally, the relevance measure of visual parts is based on the levels of the shape hierarchy on which they are determined, similarly as it is the case in Kimia et al. [11] (see also [16]). Thus, we can obtain a relevance measure together with object parts. In contrary, part decomposition based on points of minimal negative curvature is binary, i.e., the obtained parts cannot be distinguished according to their salience.

Our shape decomposition corresponds to the hierarchy of parts based on the evolution of shocks in the entropy scale space in Kimia et al. [11]. As argumented in [11], the evolution of shocks requires not only boundary, but also region information. However, observe that our part decomposition requires only boundary information. This means that our approach to shape decomposition allows us to obtain the region information from the evolution hierarchy of the boundary curve. Thus, boundary information plus evolution hierarchy is sufficient for partitioning of a two-dimensional shape.

3 Curve Evolution by Linearization

The presented curve evolution method by linearization has been applied to digital simple closed 8-curves. We have used a watershed segmentation algorithm that automatically produces such curves as boundary curves of digital objects in real images.[1] Therefore, our curve evolution as well as the shape decomposition algorithms can be applied to real images. This is demonstrated in Figure 6.

First the original image (a) is segmented using color and texture segmentation in Pauwels et al. [18]. The watershed algorithm applied to the segmented rabbit image (b) produces the object contour (c) that is a simple closed 8-curve. In (d), (e), (f), we see a few stages of the curve evolution. The obtained evolution hierarchy (f)>(e)>(d) yields the illustrated decomposition into visual parts.

In the first step of our curve evolution method, a digital curve is divided into maximal digital line segments. The decomposition of a digital curve into maximal line segments is based on the observation that every digital curve can be decomposed into digital line segments, even if the curve is strongly distorted by noise. We use a linear algorithm (with respect to the number of points in the curve) from Debled and Reveilles [5] to obtain a decomposition of a digital curve into maximal digital line segments. The decomposition in linear time belongs to newer achievements of digital geometry, a first linear algorithm was given 1991 by Smeulders and Dorst [19].

The process of **curve evolution by digital linearization** is very simple:

[1] This watershed algorithm was successfully applied in image segmentation for object based data representation of video sequences, see Lakämper and Seytter [12].

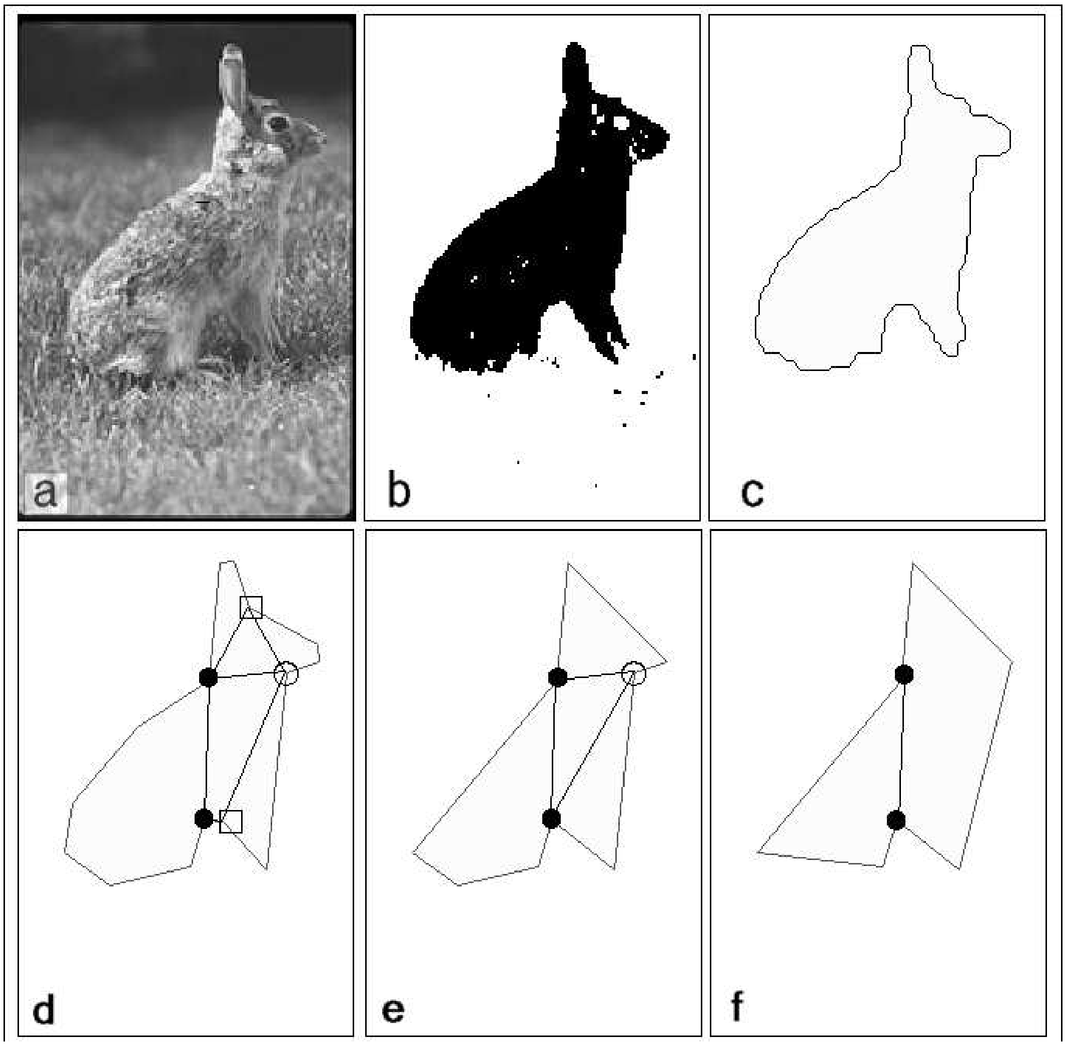

Figure 6: From an image to a simplified shape representation and to visual parts. (a) $\rightarrow$ (b): color and texture segmentation (Pauwels et al.), (b) $\rightarrow$ (c): watershed segmentation, (c) $\rightarrow$ (f): boundary curve evolution.

- The minimum of the cost function K (defined in Section 4) determines the pair of line segments that is substituted by a single line segment joining their endpoints. The substitution determines a single step of the curve evolution. We repeat this process for the new curve, i.e., we determine again the pair of line segments that minimizes the cost function, an so on.

Let $\mathcal{D}_m = s_0, ..., s_{m-1}$ be a decomposition of a digital curve C into consecutive maximal digital line segments. The algorithm that computes the decompositions $\mathcal{D}_k$ for each stage of the curve evolution $k = m, m-1, ..., 3$ until $\mathcal{D}_{k-1}$ is convex is the following:

Curve Evolution Procedure($\mathcal{D}_m$)
k = m;
Do
Find in $\mathcal{D}_k$ a pair s_i, s_{i+1} (mod k) such that $K(s_i, s_{i+1})$ is minimal;
$\mathcal{D}_{k-1} = \mathcal{D}_k$ with segments s_i, s_{i+1} replaced by the line segment s' that joints the endpoints of arc $s_i \cup s_{i+1}$;
k = k-1;
until $\mathcal{D}_{k-1}$ is convex.

This algorithm is guaranteed to terminate, since in every evolution step, the number of digital line segments in the curve decomposition decreases by one (one line segment replaces two adjacent segments). It is also obvious that this evolution converges to a convex polygon, since the evolution will reach a state where there are exactly three line segments in the curve decomposition, which clearly form a triangle. Of course, for many curves, a convex polygon with more then three sides can be obtained in an earlier stage of the evolution. Thus, we obtain

Proposition 1 *Curve evolution by digital linearization converges to a convex polygon.* ■

For many objects, the result of the presented evolution is similar to the results in Mokhtarian and Mackworth [15] and in Bruckstein et al. [2]. For example, Figure 12 shows the similarity of our evolution to the evolution in [15]. Thus, the presented evolution can also be used as basis for shape description in curvature scale space following [15]. In [15] a planar curve is convoluted with a Gaussian function with parameter σ, which leads to smoothing of a planar curve in the direction of the normal with speed proportional to curvature. This implies that relevant corners will get smoothed, even in the early stage of the evolution, which can lead to loss of important shape information. Our evolution method preserves relevant corners while at the same time it eliminates noise distortions. Since our evolution method is applied directly to a digital curve, it neither requires any curve smoothing, curve fitting nor any local curvature calculation as a preprocessing step.

Additionally our evolution method is parameter free. For evolution steps in [15] it is necessary to determine the Gaussian function parameter σ. For the newly presented muliscale curvature method in Dudek and Tsotsos [6], it is necessary to determine a *curvature tuning parameter*.

Our evolution method allows us to eliminate noise influence without changing the shape of objects, since distortions caused by noise mostly result in pairs of digital line segments that have relatively low value of the relevance measure K (presented in Section 4) when noisy boundary parts contribute in an irrelevant way to shape of a given object. The relevance order induced by K begins with pairs of arcs that contribute in the less significant way to shape of a given curve, which are arcs of relatively small length and total curvature.

Such arcs are most likely to result from noise distortions. Since they are removed in the early stages of the curve evolution, the results of the presented evolution are very stable with respect to noise. For example, although the boundary curves (2a) and (3a) in Figure 12 are distorted by noise to a large extend in various ways, the results of the evolution of curves in (1a), (2a), and (3a) are very similar. The robustness with respect to noise of our curve evolution method is also due to the fact that we are using global curvature information.

4 Relevance Order

Our evolution process is guided by a relevance order. We assign to every pair of two adjacent line segments s_1, s_2 in a decomposition of a given digital curve C a cost $K(s_1, s_2)$ which represents the significance of the contribution of arc $s_1 \cup s_2$ to the shape of C. We order pairs of adjacent line segments with respect to this significance cost. We will call this order a **relevance order**. The exact value of the cost function we used in our experiments is given by the formula (1) in Section 6. To motivate and derive this formula, we use tangent space representation of digital curves in Sections 5 and 6. In this section, we state basic requirements for the relevance order.

The linearization cost $K(a)$ of any supported arc a depends on its relative length (with respect to the curve) and its global curvature. (In particular, a pair of two adjacent line segments s_1, s_2 forms a supported arc $s_1 \cup s_2$.) Recall that we work with digital polygonal arcs. Thus, we use polygonal definitions of the global curvature, which is equal to the total turn of a polygonal arc. The definition of **global curvature** (or **total turn**) of a polygonal arc is illustrated in Figure 7. This definition has been extended to digital arcs in Latecki and Rosenfeld [13].

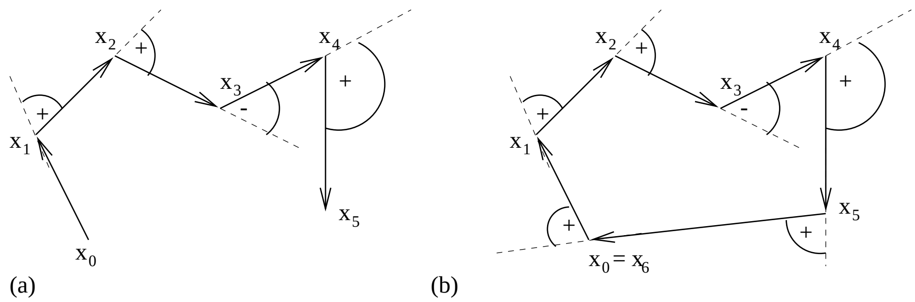

Figure 7: (a) The **total turn** of a polygonal arc is the sum of turn angles at its vertices: $\tau(x_1) + \cdots + \tau(x_4)$. (b) For a closed polygonal arc, the total turn is $\tau(x_0) + \cdots + \tau(x_5)$.

It seems that an adequate measure of the relevance of a supported arc for the shape of a given object can be based on two parameters, relative length and turn angle. We assume that the larger the relative length and the total turn of a supported arc, the greater is its contribution to the shape of a curve. Thus, the cost function K is monotone increasing with respect to the relative length and the total curvature. This assumption can be justified by the rules on salience of a limb in Siddiqi and Kimia [16]. It can be also motivated by the example objects in Figure 8 and by the experimental results described below. The bold arc in Figure 8(b) has the same turn as the bold arc in Figure 8(a) but is longer, and the bold arc in Figure 8(c) has the same length as the bold arc in Figure 8(a) but its turn is greater. While the bold arc in Figure 8(a) can be interpreted as an irrelevant shape distortion, the bold arcs in (b) and (c) are more likely to represent relevant shape properties of the whole object. As it can be easily observed, the contribution of the bold arc in Figure 8(d) to the shape of the displayed object is the most significant. This arc has the largest turn as well as the largest length.

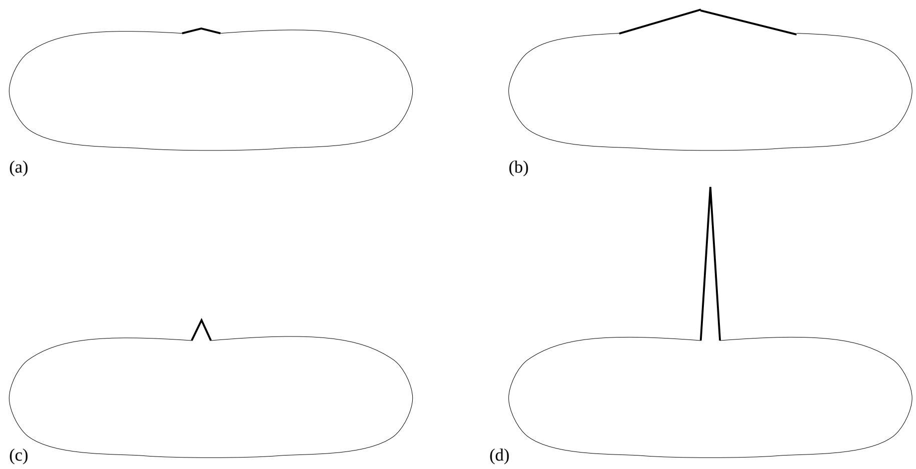

Figure 8: The influence of the bold arcs on the shape of the curve depends on their turn and length.

5 Tangent Space Representation

To derive the formula for the relevance measure, we use a *tangent space*. A digital curve C is represented in the tangent space by the graph of a step function, where the x-axis represents the arclength coordinates of points in C and the y-axis represents the direction of the line segments in the decomposition of C. For example, Figure 9 shows a digital curve (a) and its step function representation (b) in the tangent space. We will call each horizontal line segment in the graph of the step function a **step**. We traverse a digital curve in the counter clockwise direction and assign to each maximal line segment in the curve decomposition a step in the tangent space. The y-value of a step is the directional angle of the line segment and the x-extend of the step is equal to the length of the line segment normalized with respect to the length of the curve.

Formally, the **tangent space** is a torus $S_1 \times S_2$, where S_1 is a circle of length one that

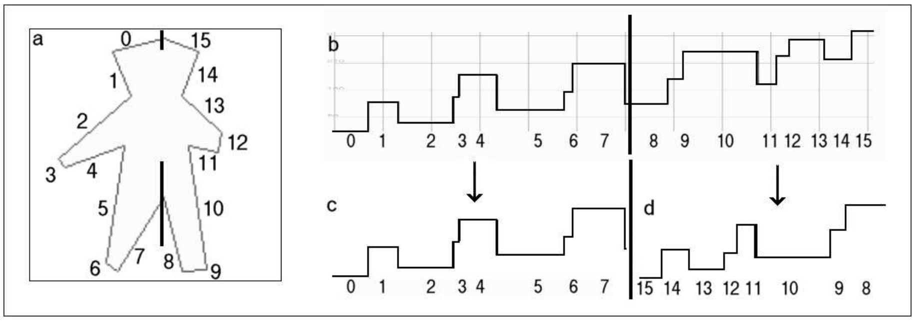

Figure 9: A digital curve (a) and its step function representation in the tangent space (b). The similarity of (c) and (d) shows that the curve (a) is symmetric.

represent the length of a digital curve and S_2 is a circle that represents the angular direction of digital line segments. We will display the tangent space as a rectangle with the parallel sides identified in the standard way to obtain a topological torus. The y-difference between two adjacent steps in the tangent space represents the turn angle of the corresponding pair of line segments. The significance of the contribution of a pair of consecutive line segments to the shape depends on their length and the turn angle in the direction of traverse. Exactly these two parameters are represented in the tangent space.

We assume that the digital plane $\mathbb{Z}^2$ is embedded in the plane $\mathbb{R}^2$ in the standard way, i.e., as a grid of points with integer coordinates. Let $C : \{p_0, ..., p_n\} \to \mathbb{Z}^2$ be a digital 8-curve with $C(p_0) = C(p_n)$ parameterized by the normalized arclength, which can be achieved by the following construction, for example:

Let $arclength(C(p_k))$ denote the distance of point $C(p_k)$ from point $C(p_0)$ measured (in $\mathbb{R}^2$) while traversing C in the counter clockwise direction. We normalize the length of curve C so that its total length is one, i.e., $arclength(C(p_n)) = 1$.

A digital curve C is traversed in the counter clockwise direction and divided into maximal digital line segments $s_1, ..., s_m$ (using a linear algorithm by Debled and Reveilles [5]).

For a line segment s in C , we define $length(s)$ to be the length of s normalized by the length of C, i.e., $length(s) = arclength(end(s)) - arclength(beginning(s))$, where $end(s)$ is the endpoint of s and $beginning(s)$ the beginning point of s. We also define $angle(s)$ to be the angular direction of line segment s in the standard coordinate system of the plane.

Now we define a transformation T mapping a digital 8-curve to the tangent space. For illustrations, see Figures 9(a) and (b). To each digital line segment $s \in \{s_1, ..., s_m\}$, a line segment $T(s)$ in the tangent space is assigned such that

$$\pi_y(T(s)) = angle(s)$$

and

$$\pi_x(T(beginning(s))) = arclength(beginning(s)), \qquad \pi_x(T(end(s))) = arclength(end(s)),$$

where π_x and π_y denote the projections on x- and y-axes in the tangent space, correspondingly. This means that y-value of all points in $T(s)$ is equal to $angle(s)$ and the projection of $T(s)$ on the x-axis has the same (normalized) arclength coordinates as s in C. This implies that the length of $T(s)$ is equal to $length(s)$.

An analytical description of the transformation to the tangent space for continuous curves can be found in Zahn and Roskies [22]. They call the step function in the tangent space a *cumulative angular bend function.* Zahn and Roskies use this transformation only as an intermediate step to obtain Fourier descriptions of planar curves. They neither use the tangent space for analyzing the underlying planar curves nor for scale transformations, which we will describe below. Uesaka [21] uses the transformation of polygonal arcs to the tangent space to determine a circular approximation of polygonal arcs.

6 Relevance Measure

For each two adjacent line segments s_1, s_2 in the decomposition of a digital curve C, we determine the relevance measure $K(s_1, s_2)$, which represents the significance of the contribution of arc $s_1 \cup s_2$ to the shape of C. The value $K(s_1, s_2)$ can be interpreted as the cost required for linearization of arc $s_1 \cup s_2$.

Let $s_1 = AB$ and $s_2 = EF$ be two consecutive line segments in the decomposition of curve C, such that $B = E$ is their common endpoint (see Figure 10) and $\beta = \beta(s_1, s_2)$ is the turn angle, i.e., $angle(EF) - angle(AB) = \beta$ (where $angle(s)$ represents the angular direction of line segment s). We determine the circular arclength by which the endpoints B and F must be rotated around points A and E, correspondingly, so that the rotated line segments have the same direction, i.e., until AB' and EF' are parallel, where B' and F' are the images of B and F by the rotations. The circular arclength must be equal for both line segments. The cost function K assigns to pair s_1, s_2 this circular arclength. We will show below that it is given by the formula

$$K(s_1, s_2) = \frac{\beta(s_1, s_2) l(s_1) l(s_2)}{l(s_1) + l(s_2)}, \tag{1}$$

where l is the length function normalized with respect to C.

Without loss of generality, we can assume that $angle(EF) - angle(AB) = \beta > 0$. We seek an angle x, $0 \leq x \leq \beta$ such that

$$angle(s_1) + x = angle(s_1) - (\beta - x) \tag{2}$$

and

$$l(s_1)x = l(s_2)(\beta - x). \tag{3}$$

Equation (2) expresses that line segments s_1 and s_2 have the same angular direction after the rotations. Equation (3) expresses that their endpoints must be rotated by the same

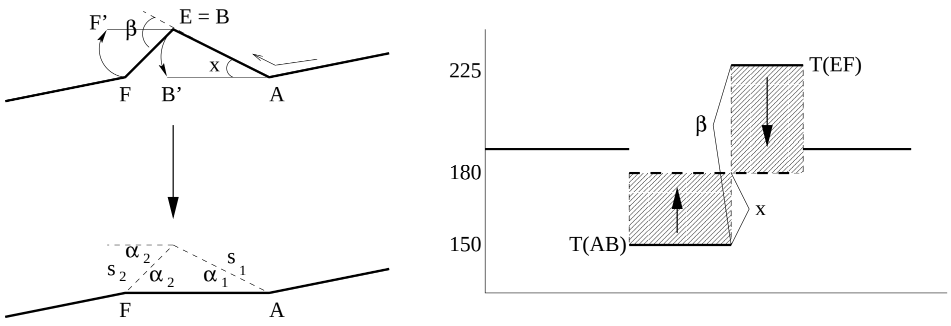

Figure 10: Scale transformation in the tangent space.

circular arclength. The pair of equations (2) and (3) can be interpreted in the tangent space (see Figure 10(right)) as translation of steps $T(s_1)$ and $T(s_2)$ parallel to y-axis until they have the same (angular) y-value and the rectangles obtained by their moves have the same area. By simple calculation, we obtain $x = \frac{\beta l(s_2)}{l(s_1)+l(s_2)}$, and consequently, by (3), the circular arc length is equal to (1).

The cost function in (1) is our measure of how significant is the contribution of a pair of consecutive line segment to the shape of the curve. The minimum of the cost function determines the pair that is substituted by a single line segment joining their endpoints, which results in a single step of curve evolution, e.g., if K obtains the minimum for line segments AB and EF, then they are deleted from C and the new line segment AF is added to C. The result of substituting the segments AB and EF with segment AF is shown in Figure 10(left).

The tangent space representation is transformed in the corresponding way (see Figure 10(right)): the steps $T(AB)$ and $T(EF)$ are deleted and a new step $T(AF)$ is added. Since it is not sufficient to represent the length of the new step $T(AF)$ by $l(s_1) + l(s_2)$, we take the length of digital segment AF as the length of step $T(AF)$, i.e., the length of $T(AF)$ is equal to

$$l_{AF} = \sqrt{l(s_1)^2 + l(s_2)^2 + 2l(s_1)l(s_2)\cos\beta}.$$

Examples of the curve evolutions together with the corresponding transformations of the tangent spaces are shown in Figures 13 and 14.

The value (1) of the cost function determines the rotations of line segments s_1 and s_2 until they are parallel. In the process of curve evolution, the segments s_1 and s_2 are substituted by a line segment s' joining the endpoints of $s_1 \cup s_2$. In the following, we show that the rotations yield an equivalent change of curve C as substitution of segments s_1 and s_2 by s' if the rotations angles are *small*. This also justifies the interpretation of $K(s_1, s_2)$ as the cost required for linearization of arc $s_1 \cup s_2$.

We recall that $s_1 = AB$ and $s_2 = EF$ are two consecutive line segments in the decomposition of curve C, such that $B = E$ is their common endpoint (see Figure 10). We rotated segment EF around point E so that the length of circular arc FF' is given by formula

(1). Now we change the interpretation of this rotation (see Figure 11): we rotate EF around point F so that the length of arc drown by E is given by formula (1), i.e., the length of circular arc EE' is given by formula (1). We will show below that the rotated segments AB' and FE' must be contained in $s' = AF$ if the rotations angles are *small.*

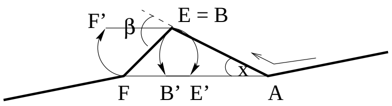

Figure 11: The rotated segments AB' and FE' must be contained in $s' = AF$ if the rotations angles are *small.*

Precisely, we will show that the segments obtained by the rotation of AB and EF, around points A and F, correspondingly, are located *very close* to AF if angles $\alpha_1 = BAF$ and $\alpha_2 = EFA$ are *small* (see Figure 11).

Small means here that $\sin(\alpha_1) \approx \alpha_1$ and $\sin(\alpha_2) \approx \alpha_2$, which is usually assumed for angles less than some γ in the interval $[\frac{\pi}{12}, \frac{\pi}{9}]$, depending on the required accuracy.

Since the rotation angle of a line segment around one of its endpoints is the ratio of the circular arc length drown by the other endpoint during the rotation to the length of the segment, we obtain from Eq. (1) that the rotation angles for segments AB and EF are

$$x = w_1 = \frac{\beta l(s_2)}{l(s_1) + l(s_2)} \qquad \text{and} \qquad w_2 = \frac{\beta l(s_1)}{l(s_1) + l(s_2)}.$$

By the sinus formula

$$\frac{l(s_1)}{\sin \alpha_2} = \frac{l(s_2)}{\sin \alpha_1}, \quad \text{we have} \quad \frac{l(s_1)}{\alpha_2} \approx \frac{l(s_2)}{\alpha_1}.$$

Since $\beta = \alpha_1 + \alpha_2$, it can be easily calculated that

$$\frac{\beta l(s_2)}{l(s_1) + l(s_2)} \approx \alpha_1 \qquad \text{and} \qquad \frac{\beta l(s_1)}{l(s_1) + l(s_2)} \approx \alpha_2,$$

which implies that

$$w_1 \approx \alpha_1 \qquad \text{and} \qquad w_2 \approx \alpha_2.$$

This means that segments AB and EF after rotation by angles w_1 and w_2 around points A and F, correspondingly, will be nearly contained in the segment AF. Since we deal with digital segments, the approximation accuracy can be calculated with respect to resolution of the square grid. We will not discuss this subject here, it is related to the sufficient digitization resolution (see Gross and Latecki [7]).

Since the values of the cost function can be defined in the tangent space, which is a torus, the presented evolution method is rotation invariant. Since the curve length is normalized, the evolution is scaling invariant. Since the minimum of the cost function does not depend on the direction and order of the traversal of line segments, the evolution is reflection invariant. It can be easily seen that it is also translation invariant.

7 Future Work

The presented tangent space allows us to reduce the complexity of symmetry detection in presence of noise and occlusions, which is a complicated task (see e.g., see Tek et al. [20]). The symmetry of some boundary parts of a given object can be detected given the step function representations of the boundary curve:

If boundary part A is a symmetric image of part B, then the step function of A is equal to the point reflection of the step function of B.

For example, the point reflection of part 8–15 of the step function in Figure 9(b), shown in (d), is equal to part 0–7, shown in (c).

Our approach also allows us to describe a similarity measure for digital arcs. The hierarchical shape decomposition and the relevance measure for convex arcs make possible to define a similarity measure for planar objects. This measure can be applied for automatic object indexing and search in image data bases, since the newest advances in automatic object segmentation (e.g., [18]) make it possible to automatically extract objects of interest for some relevant classes of digital images (see e.g., Figure 6). These topics as well as a 3D version of our results will be treated in forthcoming papers. While our 2D evolution by digital linearization is length minimizing, the 3D analog is area minimizing.

8 Acknowledgments

The work of Longin Jan Latecki was supported by the project Ec 170/1-1 from the German Research Foundation (DFG). We greatly appreciate the help of Prof. Ulrich Eckhardt (Institut für Angewandte Mathematik, Universität Hamburg) and Prof. Hans-Joachim Kroll (Mathematisches Institut, Technische Universität München), who made this project feasible. We also appreciate helpful comments and advice from Prof. Ulrich Eckhardt.

References

[1] D. H. Ballard and Ch. M. Brown. *Computer Vision.* Prentice-Hall, Englewood Cliffs, NJ, 1982.

[2] A. M. Bruckstein, G. Shapiro, and C. Shaked. Evolutions of Planer Polygons. *Int. J. of Pattern Recognition and Artificial Intelligence* 9, 991–1014, 1995.

[3] J. Beusmans, D. D. Hoffman, and B. M. Bennett. Description of solid shape and its inference from occluding contours. *Journal of the Optical Society of America* A. 4, 1155–1167, 1987.

[4] H. Freeman. Shape description via the use of critical points. *Pattern Recognition* 10, 159-166, 1978.

[5] I. Debled and J.-P. Reveilles. A linear algorithm for segmentation of digital curves. *Parallel Image Analysis and applications. Series in Machine Perception and Artificial Intelligence* 19, 73–100, World Scientific, 1996.

[6] G. Dudek and J. K. Tsotsos. Shape Representation and Recognition from Mutliscale Curvature. *Computer Vision and Image Understanding* 68, 170–189, 1997.

[7] A. Gross and L. Latecki. Digitizations Preserving Topological and Differential Geometric Properties. *Computer Vision and Image Understanding* 62, 370–381, Nov. 1995.

[8] A. Gross and L. J. Latecki, A realistic digitization model of straight lines, *Computer Vision and Image Understanding* 67, 131–142, 1997.

[9] D. D. Hoffman and W. A. Richards. Parts of Recognition. *Cognition* 18, 65–96, 1984.

[10] D. D. Hoffman and M. Singh. Salience of visual parts. *Cognition* 63, 29–78, 1997.

[11] B. B. Kimia, A. R. Tannenbaum, and S. W. Zucker. Shapes, shocks, and deformations, I: The components of shape and the reaction-diffusion space. *Int. Journal of Computer Vision* 15(3), 189-224, 1995.

[12] R. Lakämper and F. Seytter. Manipulation objektbasiert codierter Bilder als Anwendungsbeipspiel neuer Videostandards. *Proc. of DAGM Conf. on Pattern Recognition (Mustererkennung)*, Braunschweig, 427–434, Springer 1997.

[13] L. J. Latecki and A. Rosenfeld. Supportedness and Supportedness: Differentialless Geometry of Plane Curves. CAR-TR-838, Center for Automation Research, Univ. of Maryland, College Park, September 1996; also *Pattern Recognition*, to appear.

[14] R. A. Melter, A. Rosenfeld, and P. Bhattacharya (eds.), Vision Geometry. *Contemporary Mathematics.* American Mathematical Society, Vol. 119, 169–195, 1991.

[15] F. Mokhtarian and A. K. Mackworth. A Theory of Multiscale, Curvature-Based Shape Representation for Planar Curves. *IEEE Trans. Pattern Analysis and Machine Intelligence* 14, 789–805, 1992.

[16] K. Siddiqi and B. B. Kimia. Parts of Visual Form: Computational Aspects. *IEEE Trans. Pattern Analysis and Machine Intelligence* 17, 239–251, 1995.

[17] K. Siddiqi, K. Tresness, and B. B. Kimia. Parts of Visual Form: Ecological and Psychophysical Aspects. *Proc. of the IAPR's International Workshop on Visual Form*, Capri, 1994.

[18] E. J. Pauwels, P. Fiddelaers, and F. Mindru. Fully Unsupervised clustering using center-surround receptive fields with applications to colour-segmentation. *Proc. of 7th Int. Conf. on Computer Analysis of Images and Patterns*, Kiel, 17–24, 1997.

[19] A. W. M. Smeulders and L. Dorst. Decomposition of Discrete Curves into Piecewise Straight Segments in Linear Time. In [14], 169–195, 1991.

[20] H. Tek, P. A. Stoll, and B. B. Kimia. Shocks From Images: Propagation of Orientation Elements. *Proc. of IEEE Conf. on Computer Vision and Pattern Recognition*, Puerto Rico, 839-845, 1997.

[21] Y. Uesaka. A New Fourier Description applicable to open curves. *Trans. on IECE Japan A* J67-A, 166–173, 1984 (in Japanese).

[22] C. T. Zahn and R. Z. Roskies. Fourier Descriptors for Plane Closed Curves. *IEEE Trans. on Computers* 21, 269–281, 1972.

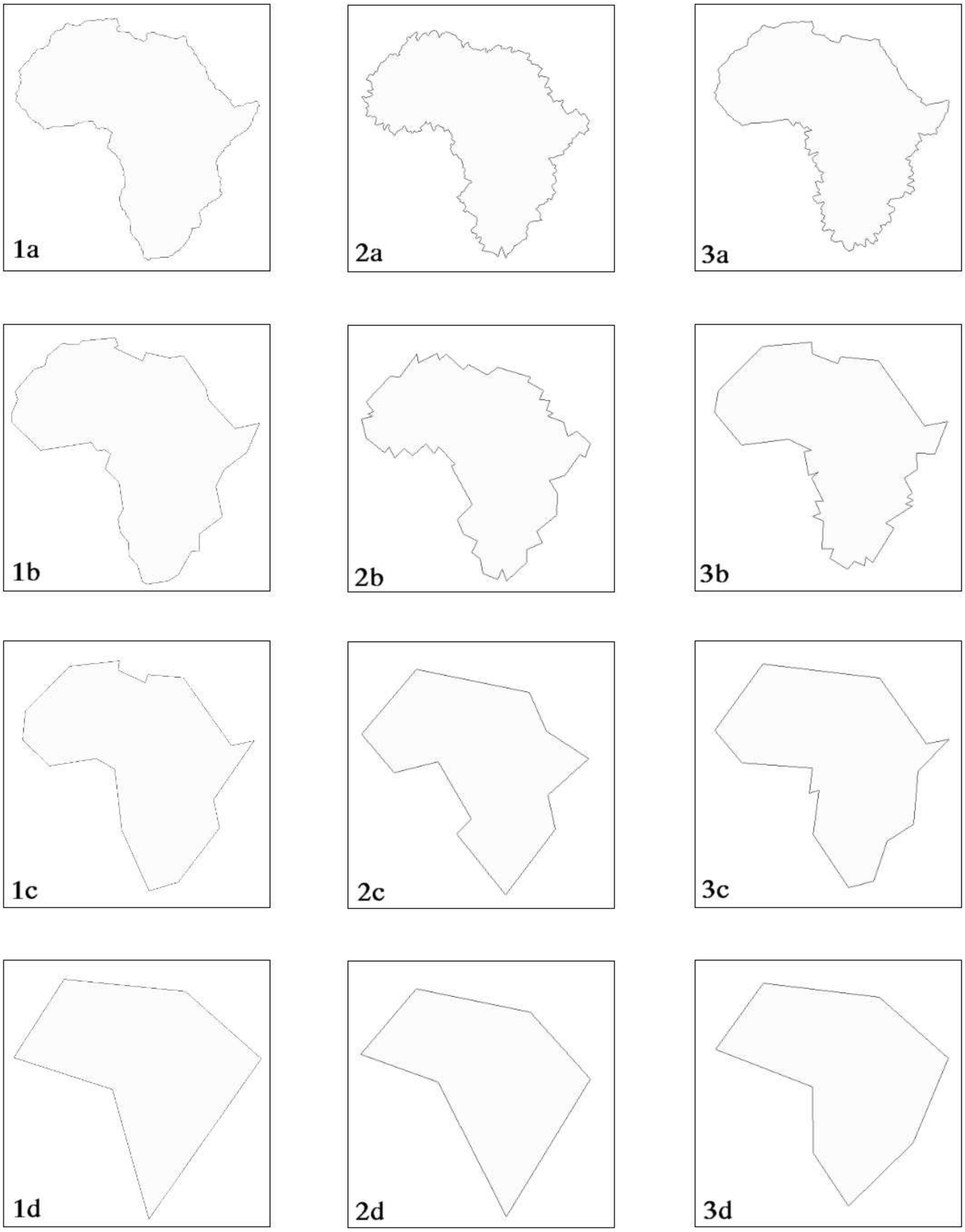

Figure 12: Shape evolution by a repetitive linearization.

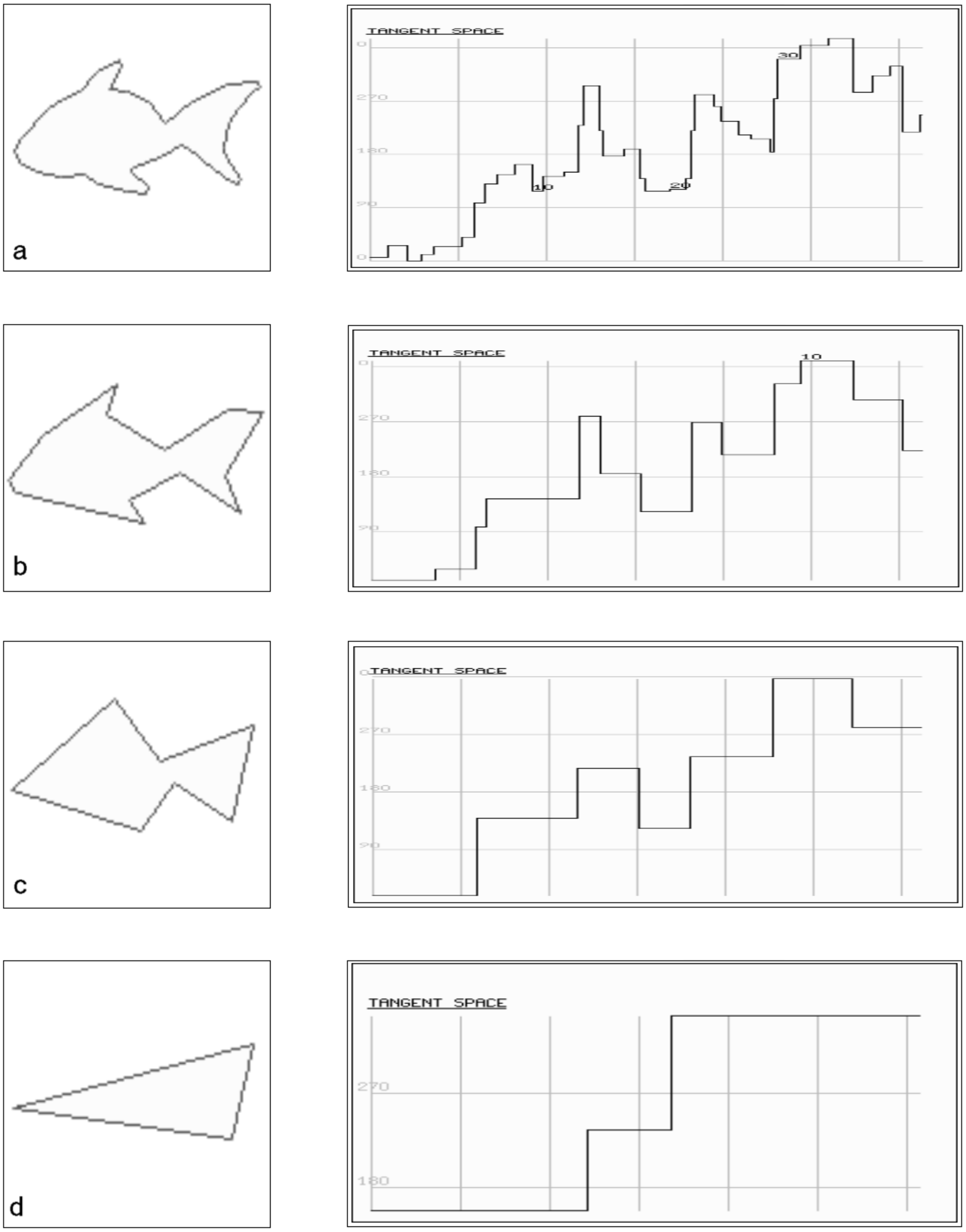

Figure 13: Shape evolution by a repetitive linearization. Next to each curve, its tangent space representation.

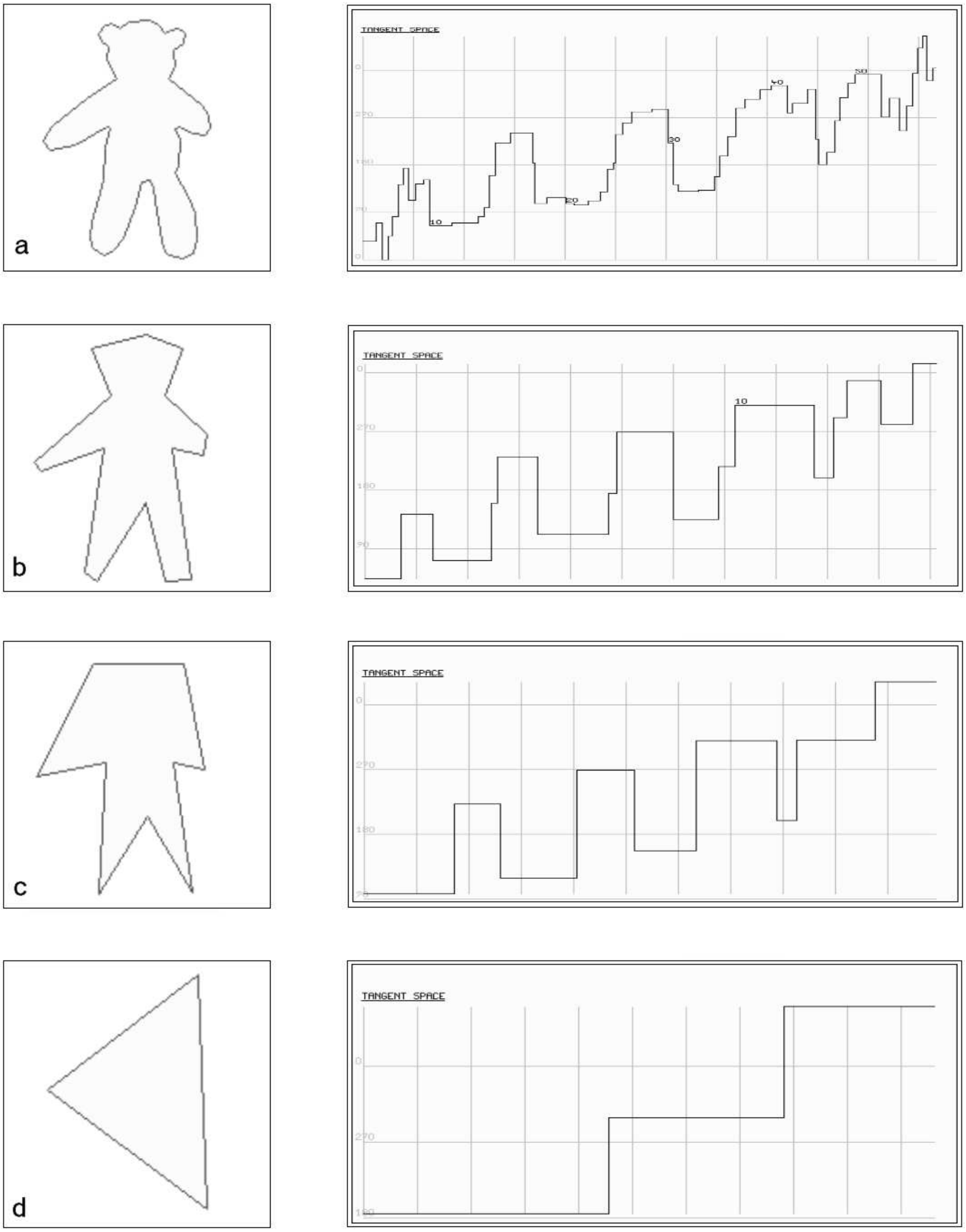

Figure 14: Shape evolution by a repetitive linearization. Next to each curve, its tangent space representation.